ARL-TR-8094 AUG 2017

US Army Research Laboratory

# Measured Visual Motion Sensitivity at Fixed Contrast in the Periphery and Far Periphery

by Paul D Fedele, Joel T Kalb, Barry D Vaughan, and Kathy L Kehring

## NOTICES

### Disclaimers

The findings in this report are not to be construed as an official Department of the Army position unless so designated by other authorized documents.

Citation of manufacturer's or trade names does not constitute an official endorsement or approval of the use thereof.

Destroy this report when it is no longer needed. Do not return it to the originator.

ARL-TR-8094 ● AUG 2017

US Army Research Laboratory

# Measured Visual Motion Sensitivity at Fixed Contrast in the Periphery and Far Periphery

**by Paul D Fedele, Joel T Kalb, Barry D Vaughan, and Kathy L Kehring**

***Human Research and Engineering Directorate, ARL***

# REPORT DOCUMENTATION PAGE

*Form Approved*
*OMB No. 0704-0188*



| 1. REPORT DATE *(DD-MM-YYYY)* | 2. REPORT TYPE | 3. DATES COVERED (From - To) |
|---|---|---|
| April 2017 | Technical Report | October 2011–October 2013 |

**4. TITLE AND SUBTITLE**
Measured Visual Motion Sensitivity at Fixed Contrast in the Periphery and Far Periphery

**5a. CONTRACT NUMBER**

**5b. GRANT NUMBER**

**5c. PROGRAM ELEMENT NUMBER**

**6. AUTHOR(S)**
Paul D Fedele, Joel T Kalb, Barry D Vaughan, and Kathy L Kehring

**5d. PROJECT NUMBER**
R.0005132.23.2

**5e. TASK NUMBER**

**5f. WORK UNIT NUMBER**

**7. PERFORMING ORGANIZATION NAME(S) AND ADDRESS(ES)**
US Army Research Laboratory
ATTN: RDRL-HRF-C
Aberdeen Proving Ground, MD 21005-5425

**8. PERFORMING ORGANIZATION REPORT NUMBER**
ARL-TR-8094

**9. SPONSORING/MONITORING AGENCY NAME(S) AND ADDRESS(ES)**

**10. SPONSOR/MONITOR'S ACRONYM(S)**

**11. SPONSOR/MONITOR'S REPORT NUMBER(S)**

**12. DISTRIBUTION/AVAILABILITY STATEMENT**
Approved for public release; distribution is unlimited.

**13. SUPPLEMENTARY NOTES**

**14. ABSTRACT**
The US Army Materiel Analysis Activity (AMSAA) Infantry Warrior Simulation (IWARS) is a constructive wargame for studying individual and small-group Soldier performance. Soldier performance depends on visual detection of enemy personnel and materiel. Vision modeling in IWARS is neither physiologically accurate nor behaviorally realistic. Movement in peripheral vision significantly influences target detection, but the IWARS visual model does not include target movement in visual detection. Monaco et al. report that most of the research in peripheral motion was conducted with limited fields of view and thus does not apply to target acquisition by dismounted Soldiers. To measure motion detection thresholds, we used targets consisting of bivariate Gaussian contrast distribution, with a Michelson contrast of –0.2 recommended by AMSAA, shaped like upright humans at ranges between 50 and 200 m and eccentricities between 40° and 80°. Measured movement thresholds were between 0.72 and 18°·$s^{-1}$, corresponding to speeds between 0.71 and 37 m·$s^{-1}$. Responses indicate that some targets could not be seen at all. These measured peripheral visual motion detection thresholds can be applied in developing a motion detection criterion supporting improved Soldier vision modeling and simulation.

**15. SUBJECT TERMS**
vision, motion, detection, threshold, periphery

| 16. SECURITY CLASSIFICATION OF: | | | 17. LIMITATION OF ABSTRACT | 18. NUMBER OF PAGES | 19a. NAME OF RESPONSIBLE PERSON |
|---|---|---|---|---|---|
| a. REPORT | b. ABSTRACT | c. THIS PAGE | | | Paul D Fedele |
| Unclassified | Unclassified | Unclassified | UU | 42 | 19b. TELEPHONE NUMBER (Include area code) 410-278-5984 |

## Contents

## List of Figures



## List of Tables

## 1. Introduction

This research supports the development of a more complete model of observer response to peripheral motion stimuli in military contexts. The objective of this project is to measure detection thresholds for visual stimuli that briefly move in the far periphery to support the development of subsequent improvements in visual target detection models. The stimuli were designed to simulate the appearance of dismounted enemy combatants moving on foot at ranges of 50–200 m. Specifically, for a set of visual eccentricities ranging from 40° to 80°, we determined the minimum speed required for a stimulus to be judged reliably as moving among a set of similar stimuli that are stationary. These data are provided in the form of 50% detection thresholds.

## 2. Background

The US Army Natick Soldier Research, Development and Engineering Center (NSRDEC) and the Army Materiel Systems Analysis Activity (AMSAA) have collaborated to develop the Infantry Warrior Simulation (IWARS) to model lethality, survivability, mobility, sustainability, and command, control, communications, computers, intelligence, surveillance, and reconnaissance during military operations. IWARS makes use of so-called intelligent agents that simulate the behavior and performance of individuals. These agents can sense changes in their environment and act based on anticipated human perception of those changes to perform tasks specified by the computer program user in a mission plan.

One such IWARS task is visual target acquisition, which includes a Soldier visually detecting, recognizing, and identifying a potential target. The Behavior Model within IWARS defines how visual search proceeds over time by means of a simple "spotlight" metaphor: A Soldier's central vision is modeled as a spatially contiguous region (a spotlight) that gathers visual information from the portion of the scene within that spotlighted region. The Behavior Model determines visual detection, recognition, and identification by spotlighting a portion of the scene and applying the process used in the ACQUIRE target acquisition model, which was first developed and applied to target acquisition using IR imaging systems (Ratches et al. 2001). The ACQUIRE model predicts the probability of detecting, recognizing, and identifying a target if one is present in the region. If a target is detected, the Behavior Model triggers the appropriate task response to the target (inspect, engage, etc.). If a target is not detected, the Behavior Model moves the

region to the next sequential portion of the scene and calls ACQUIRE again. If no targets continue to be detected, this process is continued until the entire scene has been searched, after which a new scene is selected.

The agent-based approach adopted by IWARS requires that the simulated agents perceive and behave in realistic ways for task simulation to be accurate and meaningful; the agent perception must accurately reproduce human perception over a range of perceptual conditions. In the case of human visual search, a spotlight metaphor and the application of ACQUIRE is a reasonable representation of human vision during search because the parts of the visual system primarily responsible for the human ability to perceive spatial detail, color, and stereoscopic depth are those associated with central vision.

Unfortunately, although the spotlight metaphor may be reasonable, the way the IWARS Behavior Model both defines the size of the spotlight and determines how the spotlight is directed about the scene are both physiologically inaccurate and behaviorally unrealistic. These problematic assumptions result in slow IWARS execution and unrealistic search behavior (Venezia 2009). Since battlefield target engagement is a highly time-critical and order-dependent activity, these unrealistic characterizations of target detection time and order severely limit the realism of modeled Soldier performance in IWARS.

Specifically, 2 critical aspects of human vision are poorly defined in IWARS. First, the size of the region corresponding to central vision has been fixed as a circle with a visual angle diameter of 20°. Applying a visual detection threshold over a 20° visual region is unrealistic because the high-resolution region that establishes the visual detection threshold is the highest-resolution region of the visual field: the macula, which is much smaller than 20°, is approximately 2° (Anstis et al. 1998; Brooks and Cooper 2006). The macula is the visual region required to achieve the visual threshold detection specified by the ability to resolve 3 Johnson criteria bars (Johnson 1985) over the smallest visual angle presented by the target (Brooks and Cooper 2006). While it is possible to detect a supra-detection-threshold target in a visual field larger than the macula, the detection threshold still requires use of the highest-resolution portion of the visual field, which is much smaller than the region applied in the IWARS Behavior Model.

Second, the IWARS Behavior Model fails to account for peripheral (noncentral) vision. That is, visual events outside the 20° region being assessed by ACQUIRE are invisible to the model. Events outside the 20° region have no effect on the subsequent redirection of the visual field. Humans show a highly sensitive ability to detect visual events, such as flicker, movement, and onset, in the visual periphery during visual search (Yantis and Hillstrom 1994; Yantis 1996; Rauschenberger

2003). In real-world visual search, humans use peripheral visual information to reorient their gaze toward the visual periphery, where flicker, movement, or onset has occurred during visual search (Jonides 1981). In contrast, IWARS ignores such events and always defines the progression of simulated eye movements along a fixed path from top left of the scene to bottom right, moving the way one's eyes move when reading a page of text.

Improvements in the visual characteristics of the IWARS Behavior Model could be achieved by applying a more realistic size for the central vision region where the ACQUIRE model reasonably applies the Johnson threshold detection criteria. Previous work by Monaco et al. (2010) measured degradation of visual resolution outside a central vision field approximately 8° in diameter. Targets in the Monaco et al. study were Gabor patches (sinusoidal gratings inside a bivariate, 2-D Gaussian envelope) of varying spatial frequencies. Beyond this range of eccentricity, Monaco et al. noted a decrease in perception of high-spatial-frequency information corresponding to degradation in visual acuity below 20/40, which is the prevalent minimum visual acuity standard required for driving without visual correction (TransAnalytics LLC 2003).

The improved realism afforded by the restriction of central vision to a somewhat different diameter, such as 8°, may improve model performance. The region of application of the detection threshold will be more realistic, and the number of scan regions in a field of view may be more accurately represented, but this improvement would still apply only if the Soldier actually scanned a field of view as if reading a page of text.

A more significant improvement in the visual IWARS Behavior Model could be achieved by introducing detection processes that reorient the central vision toward events, such as flicker, movement, and onset, in the visual periphery during visual search. Movement in peripheral vision has been shown to play a major part in predator detection of prey (Fouts and Nelson 1999; Ioannou and Krause 2009). Even though movement is known to attract visual attention (e.g., Yantis and Hilstrom 1994), the human visual performance model used in IWARS does not include target movement as a factor in visual detection. This change may improve the sequence of visual target detection and thus better represent real-world Soldier performance.

Monaco et al. (2007) performed an initial study to identify experimental methods for measuring the motion visibility threshold (MVT) in the far periphery. They performed initial trials using Bayesian threshold estimation procedures and new virtual reality display technology. They applied a Parameter Estimation by Sequential Testing (PEST) (Taylor and Creelman 1967) threshold estimation

procedure and measured the MVT using high-contrast black-dot targets on a bright white screen. Targets were presented at 53.4°, 72.6°, and 90° eccentricity in the temporal visual field. Measurements were reported for 2 subjects with normal visual function. Monaco et al. (2007) demonstrated that the PEST procedure could converge on MVTs within 10 yes/no stimulus trials. For the 2 subjects, the MVTs demonstrated a systematic increase with increasing eccentricity within the visual field. The average angular velocity motion thresholds MVT ($°\cdot s^{-1}$) were the following: at 53.4°, 0.5; at 72.6°, 1.35; and at 90°, 2.1 (Monaco et al. 2007).

These findings show that it is possible to obtain MVTs in the far peripheral visual field using Bayesian threshold estimation procedures that use a relatively small number of trials such as PEST.

However, sharply edged dark-black targets on a bright white screen, as used in the Monaco et al. (2007) study, are not representative of targets on the battlefield. Based on measured screen brightness used by Monaco et al., the Michelson contrast of a black target on a white screen is –0.97. Battlefield targets are intentionally made to be less visibly conspicuous. Camouflage patterns are used to break up sharp edges, and low-intensity colors are used to reduce contrast with surroundings. To better address combat-relevant visual performance, we considered different targets.

Since we wanted to isolate the influence of motion in visual detection, we chose not to use sharp-edged targets such as those traditionally used to define the Johnson visual target criteria (Johnson 1985). With such targets, a video screen representation of motion would necessarily require turning on and off specific pixels, and this process could also be detected as flash or illumination onset rather than movement. Sharp-edged targets also are subject to aliasing in digital video screen representations, and again, aliasing would create sudden pixilated incremental movements that would poorly represent smoothly moving target objects. For these reasons, we chose not to 1) use photorealistic stimuli (images of scenes, cutouts of enemy combatants and noncombatants, etc.), 2) incorporate naturalistic background scenes, or 3) represent target objects by sharply edged images.

## 3. Methods

Images often used in visual testing are designed to eliminate sharp contrast lines and aliasing in digital representations. One such type of image is the Gabor patch, which are 2-D Gaussian-shaped visibility envelopes placed over uniform sinusoidal contrast variations. Examples of Gabor patches are shown in Fig. 1.

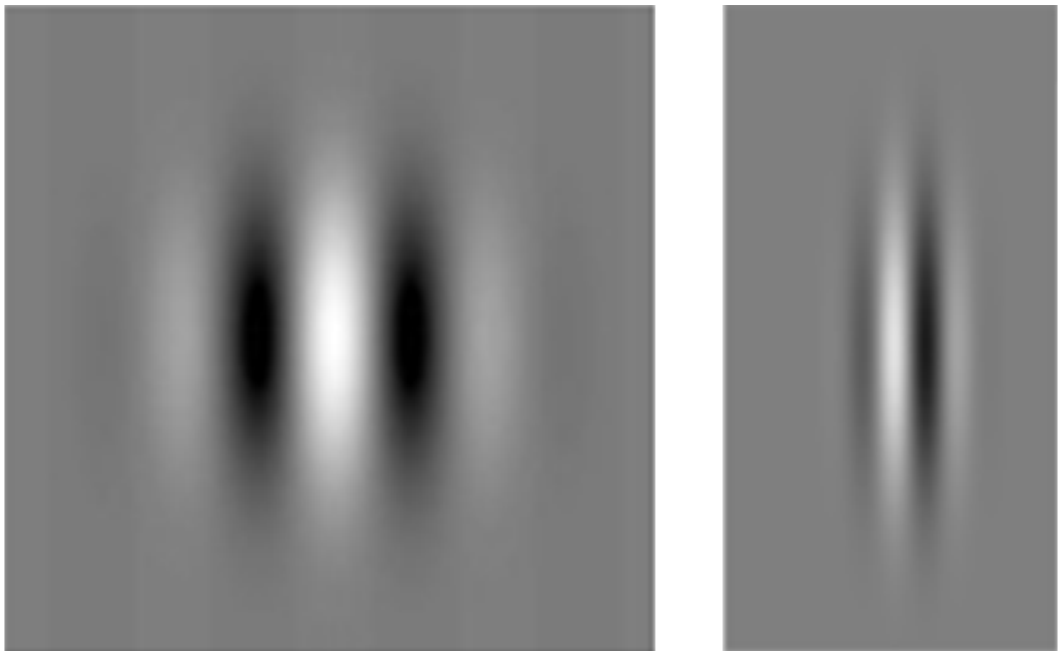

**Fig. 1 Gabor patches**

In Fig. 1, the Gabor patch on the left uses a circular Gaussian envelope in which the vertical and horizontal dispersions are equal, while the patch on the right uses an elliptical envelope in which the vertical dispersion is greater than the horizontal dispersion. Also, in the left image the envelope is centered on a point of maximum luminance, while on the right the envelope is centered on a point of average luminance.

To investigate motion detection for the human-form, we chose to use targets consisting of 2-D Gaussian-shaped contrast variations over a uniformly luminous background. Our targets used no sinusoidal luminance variations in the Gaussian window. We used only a Gaussian-shaped reduction of luminance over a background with an otherwise uniform luminance level. We approximated the form of a standing human body by using a height-to-width ratio of 4:1. Figure 2 illustrates the appearance of target images used in this study.

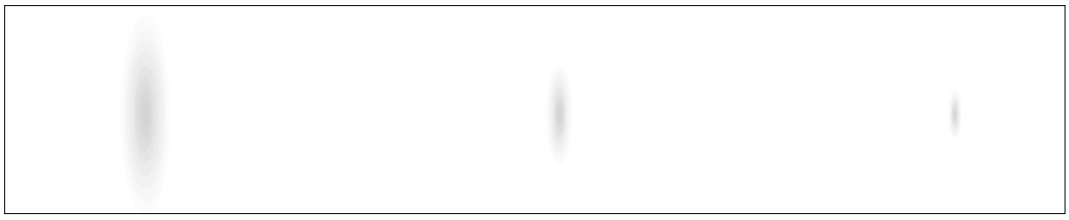

**Fig. 2 Target images used in this study**

The images in Fig. 2 are approximations of a human form at ranges of 50 (left), 100 (center), and 200 (right) m. The size of the Gaussian patch is changed to

approximate the appearance of a human form at each range. Using a Gaussian-shaped contrast variation as a target image allowed us to better isolate the detection of motion of a target of specific contrast without introducing aliasing or onset effects due to finite pixilation of the image presented on a video screen. Lateral movement of targets like those illustrated was used to measure MVTs.

Using probability functions based on successful and unsuccessful motion observation, we can empirically determine the probability that a movement in the visual periphery would be detected as a function of image angular size and eccentricity. In particular, we are interested in determining motion parameters for stimuli in the far visual periphery (greater than 45° eccentricity), as this region of the visual field has not been as well characterized historically as the near periphery (<20° eccentricity). For example, McKee and Nakayama (1984) measured peripheral motion sensitivity in the lower vision field. McKee and Nakayama demonstrated that, when normalized to units of resolvable distance per unit time, motion sensitivity remains constant for movement in the lower visual field. Since resolvable distance increases with eccentricity, their conclusion indicates that movement detection thresholds increase with eccentricity. No comparable measurements are available for the far peripheral visual field.

The following vignette defines the problem that we addressed and guided us in methodology development. A dismounted Soldier is viewing a complex visual scene in which dismounted enemy combatants may be present at ranges from 50 to 200 m. The Soldier is viewing the scene unaided by electro-optical devices or binoculars. When viewing the scene, a key indicator that an enemy is present is movement of an enemy combatant from one location to another. If movement is detected, the Soldier will reorient his gaze to the location of the movement and inspect that location more deliberately to determine if an enemy is present.

Measurements were conducted in the Tactical Environment Simulation Facility (TESF) of the US Army Research Laboratory's (ARL's) Human Research and Engineering Directorate. Targets were presented on a flat uniform gray screen.

We measured visual motion detection sensitivity at lateral eccentricities from 40°, 50°, 60°, 70°, and 80° using 3 targets with angular sizes corresponding to human targets at 50, 100, and 200 m.

The target profiles were simulated by bivariate Gaussian-shaped dark patches with standard deviations forming a height-to-width ratio of 4:1. Target images were illustrated previously in Fig. 2.

## 3.1 Participants

Sixteen individuals were recruited to participate in this study from ARL (Aberdeen Proving Ground, Maryland) between the ages of 18 and 40 with normal or corrected-to-normal vision in both eyes. Because we were investigating vision in the far periphery, participants with corrected vision were required to wear contacts rather than eyeglasses. Individuals with eyeglasses were not permitted to participate. Normal vision was defined as 20/40 or better Snellen acuity in both eyes as measured by a Titmus Model i500 test apparatus (Chester, Virginia). All subjects voluntarily provided their informed consent prior to participation, and all experimental procedures were in compliance with federal and Army regulations for the protection of human subjects (US Department of the Army 1990), as verified by ARL's Institutional Review Board. The investigator adhered to Army policies for the protection of human subjects.

## 3.2 Instrumentation

All stimuli were displayed in the TESF on an immersive 3-screen rear-projection system manufactured by Fakespace Systems (Marshalltown, Iowa; currently Mechdyne Inc., Kitchner, Canada). The 3 screens were positioned symmetrically: one screen in the center, one screen on the left, and one screen on the right, in the form of 3 sides of an equilateral hexagon. The interior angle between screens was 120°. Participants were seated 9 ft from the center of all 3 screens. An overhead view of the participant and the projection screens is shown in Fig. 3.

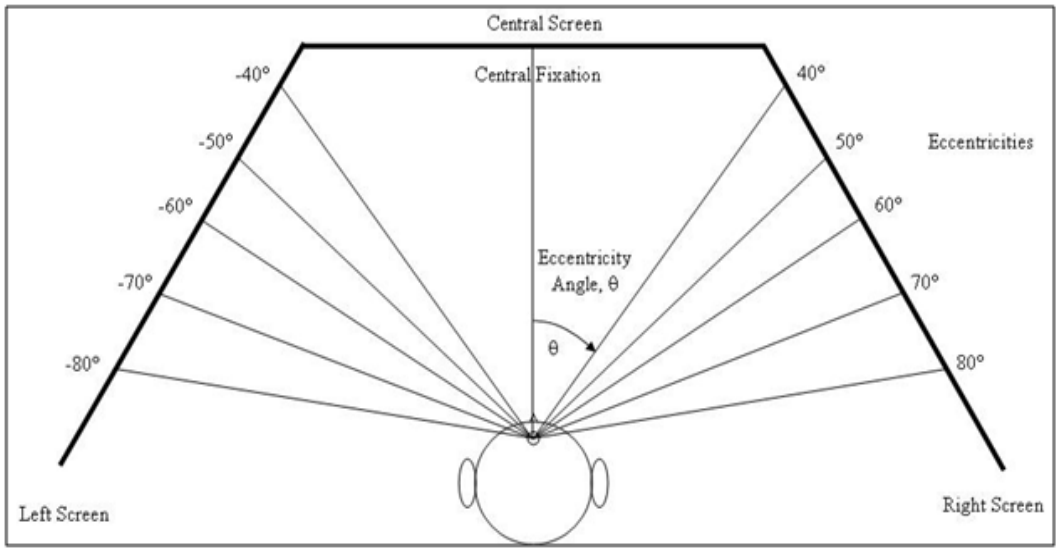


**Fig. 3 Schematic representation of screens, central fixation, and participant locations**

System images on each screen were projected by a Christie Digital 6000-lumen projector (Cypress, California) onto a 10-ft-high by 12.5-foot-wide screen. The display resolution for each screen was 1600 × 1200 pixels. At the center of each screen (i.e., at –60° and +60° eccentricities), one pixel subtended 4.3 min of arc. This value changes with eccentricity about the screen center, as we discuss when addressing movement rates in Section 3.3.

To ensure that both left and right screens presented stimuli at the same level of brightness and contrast, we performed a gamma correction procedure to linearize the luminance of the projectors. Using a Photo Research Litemate PR-525 photometer (Chatsworth, California), we measured display luminance from the observer's vantage point at the center and extreme left and right locations on each screen for every 5 grayscale levels from 0 to 254. These data were combined to produce an illuminance function for each screen. These illuminance functions provided the red-green-blue (RGB) values to be sent to the display projector to create the desired luminous contrast intensity on each projection screen.

Each screen was controlled by a separate PC running the Microsoft Windows 2000 operating system. The PCs were networked together via a Transmission Control Protocol/IP local area network isolated from all other network traffic. Custom software written in Delphi (Borland Corporation; Cupertino, California) was used to generate displays, collect participant responses, save data in Microsoft Excel format files, and ensure timing accuracy of networked PC events.

## 3.3 Test Stimuli Presentation

All test screens were filled with a uniform gray background. Experiments were conducted with a background luminance of 16 candelas per square meter ($cd/m^2$). This value is well within the photopic range of luminance (Hood and Finklestein 1986). The 3 screens produced an illuminance of 0.4 foot-candle in the test participant's facial plane. All test control stimuli and targets were presented in grayscale.

Test control stimuli consisted of a fixation cross, a trial-underway fixation cross, and text instructions including "Make your response now" and "Click the mouse for next trial". Figure 4 illustrates the appearance of the presented test control stimuli. As shown in Fig. 4, the fixation cross was a plus-sign subtending 1° of visual angle displayed on the middle screen at eye level of the seated participant. The fixation cross was displayed in black (RGB values 0,0,0). The trial-underway fixation cross was the fixation cross with a black box around it. Dimensions of the box were 1.5° × 1.5° visual angle, and it was centered at the fixation point. Text instructions were displayed on the middle screen, directly above the fixation cross,

in black Times New Roman font. The text was displayed in a size sufficient to be easily read by the observers. When the left or right choice was made, the text above the central fixation stimuli changed to read “Click the mouse for next trial”. At any time after the target movement began, or after the target movement had ended, the participant responded to the movement stimuli by using a mouse to select 1 of 2 buttons that appeared on the center screen after each trial: the left button for motion on the “left” and the right button for motion on the “right”. Participants used the mouse to begin each trial and to respond to the 2-alternative forced choice.

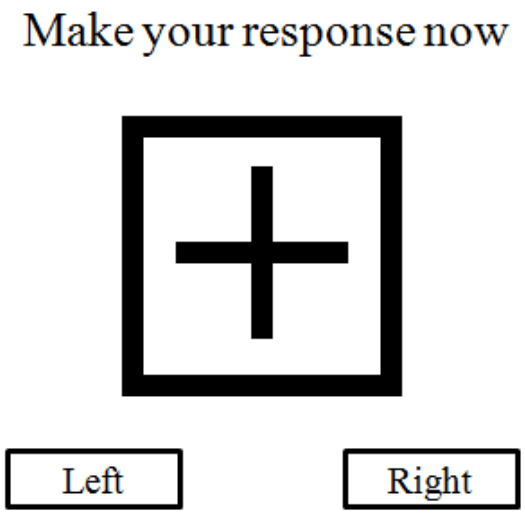


**Fig. 4 Illustration of test control stimuli (not to scale)**

Target motion-detection stimuli were arrays of images approximating the human form at various ranges and eccentricities, as shown in Fig. 2. The selection of stimuli characteristics was designed to be applicable to IWARS development needs. We selected stimuli to resemble dismounted Soldiers in both shape and luminance contrast. Discussions with personnel from AMSAA indicated that the way Soldiers are represented in the ACQUIRE target acquisition model is to have vertically oriented figures with a mean luminance approximately 50% lower (darker) than their immediate background. We chose to represent potential target stimuli as narrow, vertically oriented, bivariate Gaussian-shaped shadows.

Symmetric stimuli scenes were displayed on the left and right screens. Scenes consisted of 2 sets of 15 potential-target stimuli semi-randomly distributed across eccentricities from 40° to 80°. One set of 15 was displayed on the left screen and the other set of 15 was displayed on the right screen. Three targets were presented vertically at each eccentricity angle, one target for each simulated target range: 50 and 200 m. For each eccentricity angle, the small, medium, and large targets were randomly placed on the screen: one target centered at 5° above the horizontal plane,

one centered directly on the horizontal plane, and one centered 5° below the horizontal plane. No movement stimuli were displayed on the center screen. For all nonmoving targets, the left and right scenes were symmetric about the central fixation. Nonmoving targets were dithered horizontally at a random angle selected between ±5° about each eccentricity angle. The target to be moved was placed randomly at +5° or –5° with respect to its central eccentricity (i.e., horizontally) so it could move through a 10° arc straddling the target's central eccentricity. Dithering the nonmoving targets made it impossible to determine which target would be moved during the trial.

Figure 5 shows an illustration of one side of the target matrix for a typical motion visibility trial.

**Fig. 5 Initial target array on the full left or right screen for a typical motion-visibility trial (not to scale)**

The initial target array was mirrored on the left and right screens, symmetrically about the center of the middle screen, giving a total of 30 stimuli. During each trial, one of the 30 stimuli moved through an angle of 10°.

Although visual acuity may vary between the left and right sides, for these initial studies, results from trials when the moving target was on the left side were combined with results when the moving target was on the right side, producing a symmetric approximation of peripheral motion detection thresholds. Right side and left side responses were combined to reduce the data collection burden, and symmetry was assumed as a first approximation for vision modeling.

Each stimulus was assigned a simulated range of 50, 100, or 200 m. The height of the vertical dispersion of the target stimulus Gaussian window was a function of range as follows:

$$H = \frac{H_c\, D}{R}, \tag{1}$$

where H = height of the vertical dispersion

D = distance from participant to center of screen

$H_c$ = actual height of combatant (assumed to be 2 m)

R = simulated range from the observer to the combatant

We recognize that MVTs should depend on target contrast, so we selected a target design different from that used in the Monaco et al. (2007) study. Based on recommended military target spotting conditions recommended by AMSAA personnel, we determined the background illuminance for the screen and the minimum illuminance presented at the center of each Gabor patch target. Though there is some disagreement and a good deal of recent research examining how best to define contrast for complex objects such as Gabor patches (Peli 1997), we used a modified Michelson contrast (Peli and Arend 1993) to empirically set minimum and maximum luminance values of our Gaussian-shaped target stimuli. We specified contrast using a modified Michelson contrast given by

$$C_m = \frac{I_T - I_B}{I_T + I_B}. \tag{2}$$

In Eq. 2, $I_T$ is the target luminance and $I_B$ is the background luminance. Guidance indicated that relevant target contrast should be –0.2, so we applied a background luminance of 16 cd/m$^{-2}$ and a target luminance of 10 cd/m$^{-2}$, giving a Michelson contrast of –0.2. By comparison, a fully black target on a fully white screen, as used by Monaco et al. (2007), gives a Michelson contrast of –0.97. Using the luminance functions established for each screen, we determined the RGB values to be sent to each screen to produce uniform background luminance over each screen and uniform contrast across all targets.

Movements were produced by displacing the Gaussian pattern by a number of pixels over a number of screen-refreshes. A movement rate of one pixel for each screen-refresh was used as the basis for the range of movement rates. This pixel displacement rate corresponded to an angular target movement rate of 3.6°·s$^{-1}$. Angular movement rates were varied from a minimum of 1/10 of this amount to 10 times this amount over 40 intervals.

Movement rates were varied in decibel increments. Consistent with other sensory perception processes, we defined the movement decibel level based on the square of the ratio of angular movement rate to the rate of 1 pixel per screen-refresh. Decibel movement levels, $L_{dB}$, were determined as

$$L_{dB} = 10log_{10}\left[\left(\frac{n_{pixels/screen-refresh}}{1_{pixels/screen-refresh}}\right)^2\right] = 20log_{10}\left[\left(\frac{n_{pixels/screen-refresh}}{1_{pixels/screen-refresh}}\right)^1\right]. \quad (3)$$

Applied angular displacement rates and equivalent speeds for all target eccentricities and ranges are given in the Appendix.

In Eq. 3, the number of pixels per screen-refresh, *n*, ranged from 0.1 to 10 in decibel steps uniform in the square of the number of pixels moved per each screen-refresh. The smallest and largest movement rates used in this study were $0.36°\cdot s^{-1}$ and $36°\cdot s^{-1}$, respectively.

The targets simulated upright, dismounted humans. The range of target movement rates was selected to extend below and well above the range of possible movement rates of people on foot so that we could ensure that measured movement visibility thresholds could apply to dismounted, moving human combatants. The smallest target speed simulated by the our angular movement rate occured at the smallest simulated target range (50 m) and equals a speed of 0.31 $m\cdot s^{-1}$. The largest speed used in this study was 126 $m\cdot s^{-1}$ and corresponds with a target range of 200 m. For the shortest-range targets (50 m), the fastest target speed simulated was 32 $m\cdot s^{-1}$. A reasonable upper bound for the maximum rate at which a person can move on foot is approximately 20 $m\cdot s^{-1}$ (Weyand et al. 2000). Thus, the maximum speed used in our study was higher than a reasonable upper limit for human running speed under all of our eccentricities and simulated target ranges.

Target movement occurred over a time period not more than 750 ms and took place in the horizontal plane, either toward or away from the central fixation point. A potential confound in the study was the fact that as a stimulus moves along the horizontal line, its eccentricity necessarily changes. This confound was mitigated by limiting the duration of the movement. Also, because we modeled downrange combatants as Gabor patches, for which edges are defined by smoothly varying luminance values rather than abrupt high-low luminance changes from pixel to pixel, we could display motion at subpixel levels to simulate slowly moving targets at larger ranges.

The movement rates of target images were determined at the center of the screen and were applied, as a constant, across the entire screen. Because our target images were projected onto a flat screen, the actual angular velocity of the stimulus about the participant's view point was not constant across all eccentricities. Angular

motion rates decreased symmetrically, as eccentricities either increased or decreased, about 60°. Angular motion changed by less than 11.7% from the center of the screen to the edge of the screen, so we report motion visibility thresholds as on-screen movement rates and angular rates corresponding to the center of the side screen.

## 3.4 Procedures

For each of the 15 conditions (5 eccentricities and 3 ranges, since left and right results were combined) in the experiment, the participant performed a QUEST* (Watson and Pelli 1983; King-Smith et al. 1994) adaptive procedure to find the 50% speed threshold required to detect the moving stimuli at the ranges and eccentricities in this study. QUEST was chosen because it reduces bias and reliably converges on the 50% threshold values with only a small number of trials required (Klein 2001). For each condition (eccentricity and target range), 20 trials were conducted to allow for convergence of the QUEST procedure. Thus, each participant performed 300 total motion detection trials.

Each trial in the QUEST procedure began with the presentation of the "Click the mouse for the next trial" instruction above the fixation cross. The fixation marker remained on the screen throughout the experiment. When clicked, this instruction disappeared and the trial-underway fixation cross appeared with the elements of the simulated scene. At a random interval between 1000 and 2000 ms later, one stimulus is moved by an angle of 10°. At the start of the movement, the response prompt was displayed immediately under the boxed cross (trial-underway) fixation display, allowing the observer to respond to the movement as soon as movement could be observed. This also may have helped the subject remain focused on the central fixation point by adding change-saliency to the fixation point as the movement began. After the movement interval of 750 ms, the "Make your response now" instruction appeared over the fixation cross and the response buttons. This instruction remained on the screen until the participant made a response by clicking the left or the right response box. The participant could respond by clicking the left or right button with the mouse at any time after the stimulus movement interval had started. Responses were not rushed and response times were not collected.

Participants clicked the mouse pointer on either the right or the left response button, indicating that they felt the stimulus that moved (the target) was one of the targets displayed on the left or one of the targets displayed on the right. Participants were instructed to guess if they failed to observe motion on either side.

*Watson and Pelli (1983) dubbed as QUEST their maximum likelihood procedure for parameter estimation by sequential testing.

When the left or the right response button was clicked, the left and right screens returned to their uniform gray background, the "Click the mouse for next trial" instruction again appeared, and the next trial began upon the next mouse click. No feedback was given to participants regarding whether their response was correct.

Participants were permitted to take breaks as needed between trials by delaying pressing the mouse button when prompted to do so to begin a new trial. In addition, after 100 and 200 trials the participants were interrupted and offered a chance to take a break to relax their eyes.

Participants were told that because half of the time the movement was on the left and half on the right, their best strategy would be to keep their eyes directed toward the fixation cross. Participants also were told not to look continuously at one side. By this strategy, individuals could look only at one side and, failing to see motion on that one side, they could guess motion on the other side. This strategy would have resulted in participants not using their peripheral vision at the intended eccentricity, and the obtained data would not have represented motion detection at precise angles in the periphery and far periphery. To ensure that participants did not look exclusively at one side, participants were told they would be watched from the side. No participant appeared to be observing only a single side of the overall display, and all participants appeared to continue to look toward the central fixation throughout their trials. Participants also were told that this experiment would resolve and measure motion detection thresholds, and therefore during many trials the participant could expect to be unable to detect motion on either the left of the right side, but that they should nonetheless guess the particular side where movement may have occurred.

The adaptive QUEST procedure was used to determine the probability distribution (PD) for the MVT for each test participant at each target range and eccentricity. The QUEST process starts with an a priori assumed MVT PD. In this study, the initially assumed PD was a uniform distribution over the domain from +20 to –20 dB, with 0 dB corresponding to an angular movement rate of $3.6°\cdot s^{-1}$ ($0.063\ rad\cdot s^{-1}$). This single angular movement rate corresponds to a target velocity that depends on target range. At target ranges of 50, 100, and 200 m, target velocities corresponding to 0 dB are 3.2, 6.3, and 12.6 m/s, respectively. The final determined MVT value is the average over the final MVT PD. This average is the threshold movement rate where a person is expected to see, or detect, movement in half of all equal movement presentations.

QUEST trials were started by presenting a stimulus at a movement rate at the center of the domain of the initially assumed MVT PD. If the initial trial response is correct, the PD is modified by multiplying it, at each point, by the probability of a

correct response if the actual MVT equaled that point in the domain. Alternately, if the response is not correct, the PD is modified by multiplying it by the probability of an incorrect response if the actual MVT equaled the value at that point in the domain. Subsequent trials are conducted by presenting a stimulus at the expectation value (average) of the PD resulting from the previous modification. After each trial response, the threshold PD is again adjusted, based on whether the response was correct or incurrent. If the response is correct, the threshold PD is again modified by the probability of getting a correct response for each possible threshold value in the domain. If the response is incorrect, the threshold PD is again modified by the probability of getting an incorrect response for each possible threshold value in the domain. The trial-response-modification process is repeated a total of 20 times for each combination of range and eccentricity. The expectation value of the MVT PD after the 20th trial is taken as the resulting threshold.

With 20 trials, the final response is expected to be within 5 dB or less of the actual threshold (Klein 2001). We verified Klein's finding by using Monte Carlo simulations of experimental results. We also used the simulations to illustrate expected QUEST results to obtain greater understanding of the results of our experimental trials.

An example of a Monte Carlo simulation showing convergence of the QUEST procedure is shown in Fig. 6.

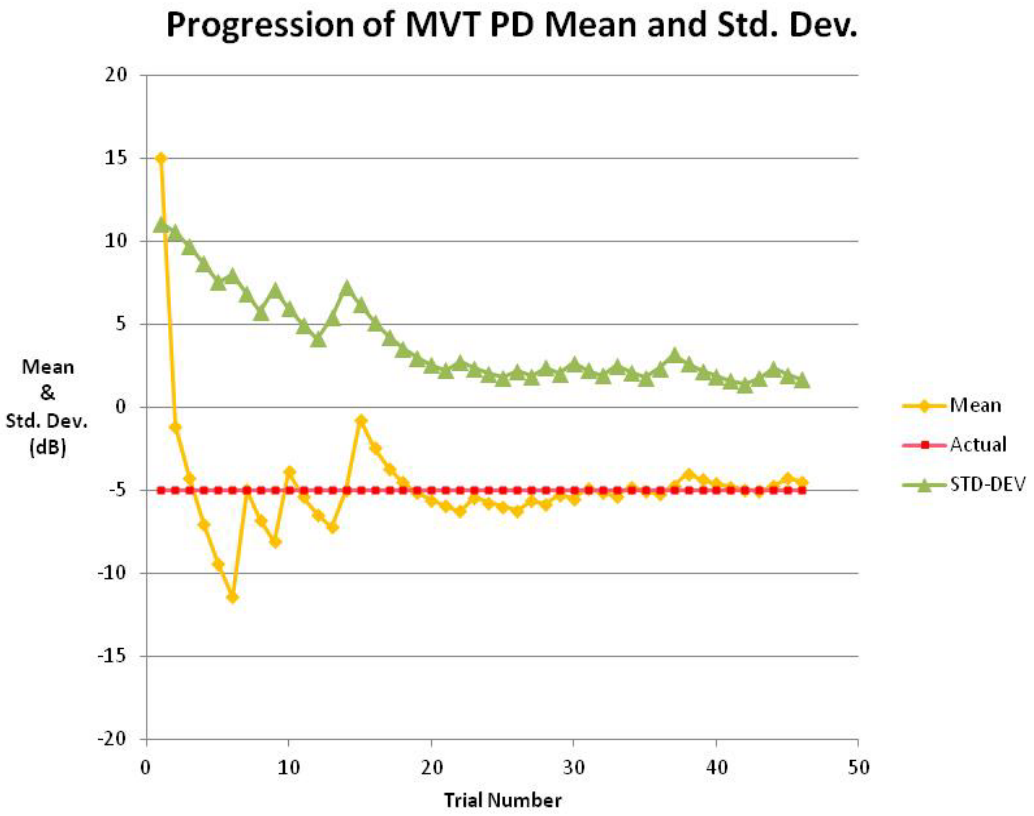


**Fig. 6 Mean and standard deviation of the PD for the MVT in successive QUEST trials in which the actual 50% threshold is –5 dB**

Starting with a uniform rectangular PD for the MVT, we simulated responses using a psychometric function 50% threshold of –5 dB and a slope of 0.2. When the response was correct, the next trial was conducted with a slower movement rate, and when the response was not correct, the next trial was conducted with a faster movement rate. As the example in the Fig. 6 shows, the mean of the MVT PD converged to within 5 dB of the actual value (–5 dB) within 20 trials. Figure 6 also shows that the standard deviation of the MVT PD converged to a stable value after 20 trials.

To demonstrate the reliability of this convergence, we simulated 250 experimental trials using an actual threshold value of –5 dB, a psychometric function slope of 0.2, and an initial stimuli guess of 15 dB. A total of 250 MVT PD means were calculated and are plotted in the histogram in Fig. 7.

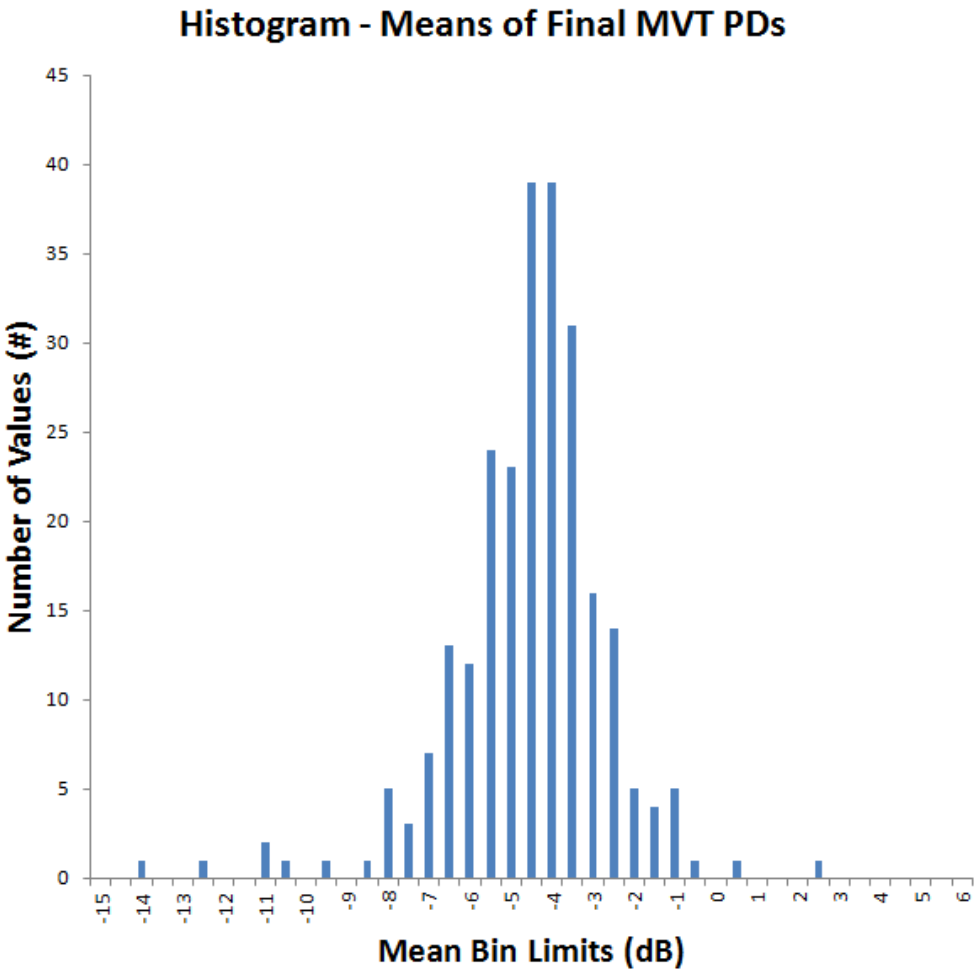


**Fig. 7 MVT PD mean values from 250 simulated experimental trials**

All histograms in this report were plotted with Microsoft Excel 2013. The bin width used in this histogram is 0.5 dB. The first bin on the left (the bin above –15 dB) contains the number of results less than –15.0 dB. There are no results less than –15.0 dB. The second bin from the left contains the number of results equal to or greater than –15.0 dB and less than –14.5 dB, which again contained no results. The third bin contains values equal-to-or-greater than –14.5 and less than 10.4 dB. One result value is in this bin, and so on.

The average value of the means in Fig. 7 is –4.79 dB. The standard deviation of the means is 1.92 dB. This demonstrates that the applied QUEST procedure reliably converges on the actual MVT to within 5 dB in 20 trials. Of the 250 trials, 7 produced results outside of the –10.0- to 0-dB range. Thus, the probability, P, of convergence within the ±5-dB range is P = (250–7/250) = 0.972, or better than 97%.

Watson and Pelli (1983) indicate that this QUEST procedure will converge toward the highest value in the domain if the actual threshold is out-of-range higher than the upper domain limit, and that the QUEST procedure will converge toward the lowest value in the domain if the actual threshold value is out-of-range below the lower domain limit.

To verify this out-of-range behavior in our QUEST implementation, we simulated trial results with an actual threshold value of +25 dB, which is above the range between –20 and +20 dB. This simulates the situation when, for example, a test participant cannot see any motion within the entire domain of movement rates or cannot at all see the target at a given eccentricity. In such cases, the QUEST procedure converged to the maximum movement rate in the experiment, verifying Watson and Pelli's finding in our QUEST implementation.

Simulating 100 experimental trials with an actual threshold value of 25 dB, a psychometric function slope of 0.2 and an initial stimuli guess of 5 dB, the simulation produced the MVT PD mean values shown in Fig. 8.

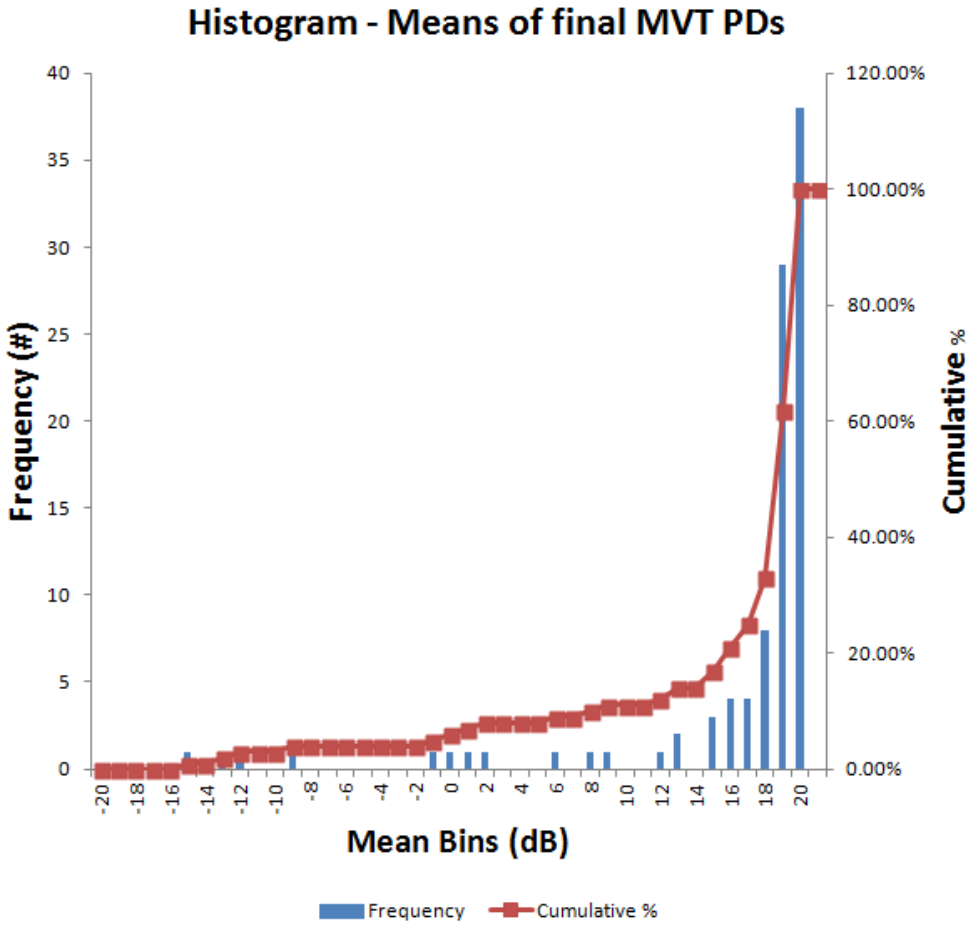


**Fig. 8 MVT PD means with an out-of-range actual threshold value of 25 dB**

The bin width in the histogram in Fig. 8 is 1 dB, and the first bin (the bin above –20) contains the number of results less than –20 dB; the second bin contains the number of results equal to or greater than –20 dB and less than –19 dB. Figure 8 shows that the QUEST procedure converges on the maximum motion rate used in the study when the actual MVT is above the experimental domain. The average value of the means in Fig. 8 is 16.0 dB. The standard deviation of the means is 7.4 dB. The distribution in Fig. 8 is neither normal nor symmetric. Over 50% of the values are greater than 18 dB. Figure 8 demonstrates that large numbers of MVT means concentrated at the endpoints of the experimental motion domain indicate that actual MVT values may be outside of the experimental motion domain or that the participant could not see the target at all, regardless of the target's movement. When the target cannot be seen at all, the actual MVT may be undefined because the target cannot be seen regardless of its movement.

Our simulation trials demonstrate that the 20-trial QUEST procedure converges closely to the actual MVT when the MVT is within the experimental motion domain, and it converges on the extreme value of the motion domain when the MVT is out of range, beyond the limits of the experimental domain. Therefore, in interpreting our experimental results, experimental values greater than 15 dB, and by symmetry less than –15 dB, may not represent actual MVT values.

To illustrate the out-of-range behavior in test participant results, we show the results produced by human subject test participant (TP) number 10. Significant variability was observed between different individuals. The results achieved by TP 10 are used to clearly illustrate the out-of-range behavior.

The results from TP 10 are shown in Fig. 9. The data format is summarized in the figure legend.

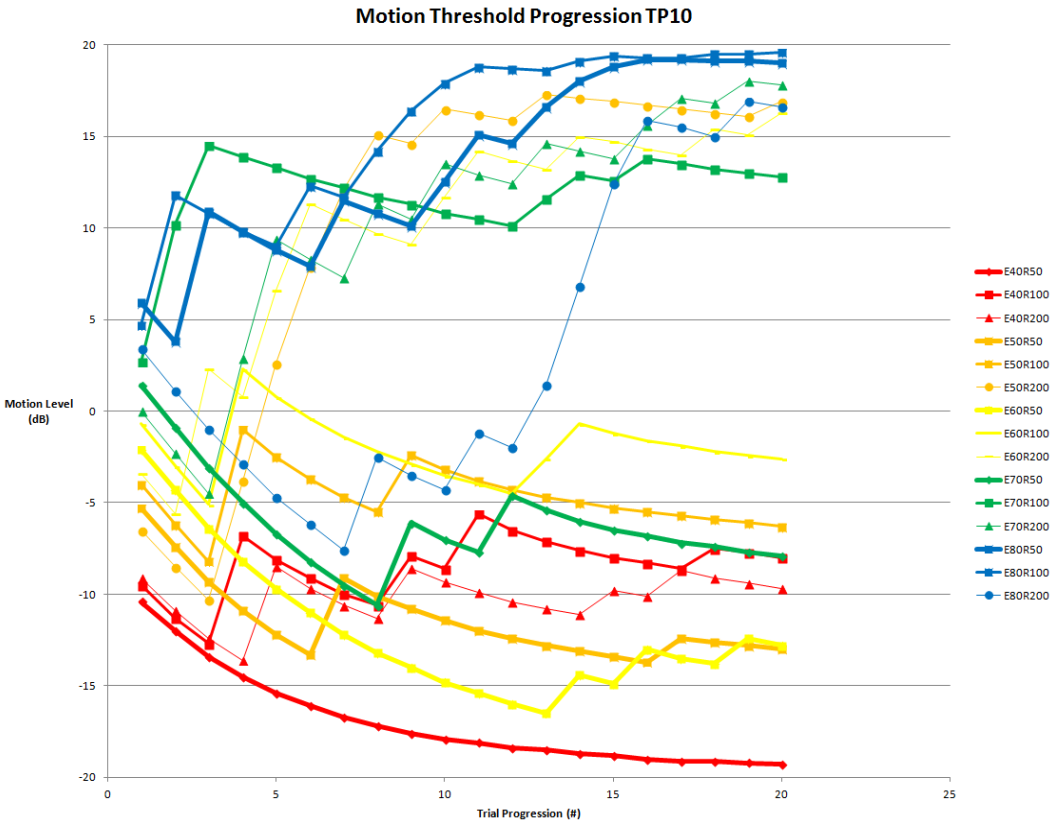


**Fig. 9 Example of MVT progression for TP 10: a specific color represents a specific eccentricity and a specific line thickness represents a human-form target viewed at a specific range. In the legend, eccentricities are given in degrees following the letter "E", and range is given in meters following the letter "R".**

In Fig. 9, lines of one color represent measurements at a particular eccentricity, while lines of the same thickness represent a particular range. The thickest line represents targets simulating a range of 50 m, while the thinnest line represents targets simulating a range of 200 m. The 5 eccentricity values are represented by different colors: red, 40°; orange, 50°; yellow, 60°; green, 70°; and blue, 80°. In the legend, the letter E denotes eccentricity, and the number following the letter E is the eccentricity in degrees. The letter R denotes range, and the number following the R is the simulated range of the target in meters.

We refer to experimental conditions as (E#, R#) in the legend of Fig. 9 and in the text. For example, we label experimental condition as E40R50, indicating an eccentricity of 40° and a simulated range of 50 m.

A collection of MVTs in Fig. 9 is above 15 dB. We consider these values to represent conditions where the actual MVT values may be above our experimental domain or may be nonexistent. Also, for (E40, R50) the test participant never made

an incorrect choice of the side where the motion occurred. We consider that the actual MVT for (E40, R50) may be below the lowest movement rate used in this study.

Our simulations show that trial results generally progress to steady values; however, such behavior is not always observed. Final values can continue to change if the observer experiences increasing fatigue or eye strain as the iterations continue. Although participants were allowed and encouraged to take breaks during the trials, we cannot ensure that fatigue was never a factor in our data.

In addition, the QUEST procedure does not produce a limiting value equal to the actual MVT as the number of iterations increases toward infinity. When a stimuli is presented at the actual MVT value, the probability of correctly observing the stimuli (P = 0.5) equals the probability of incorrectly missing the stimuli (P = 0.5). As we have shown, the QUEST procedure, however, gives an estimate of the MVT to within 5 dB after 20 iterations. The QUEST result continues to randomly fluctuate about the MVT, as trials continue, regardless of how many iterations are conducted beyond 20 iterations.

MVT results have been graphed for TP 10 as a function of both eccentricity and range, as shown in Fig. 10, which shows the MVT surface for all eccentricity and range values, illustrating the shape of the threshold surface as a function of eccentricity and simulated target range.

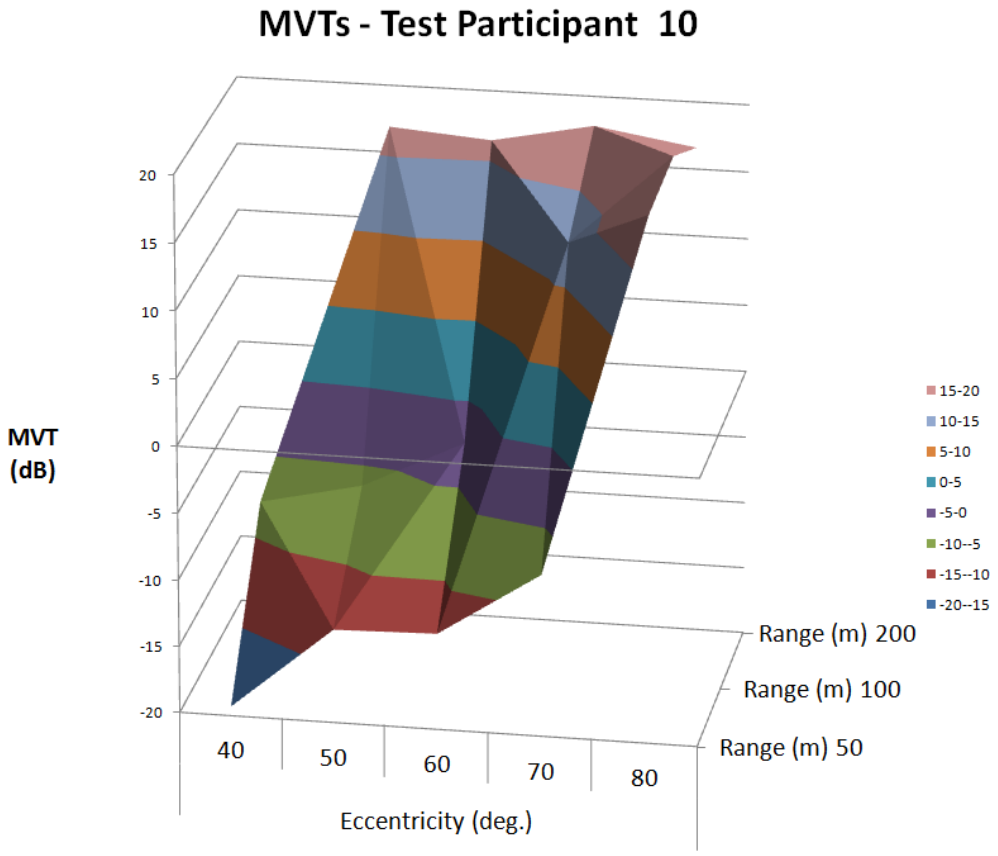


**Fig. 10 MVTs for TP 10 vs. eccentricity and range**

## 4. Overall Results

All individual MVT values—all eccentricities and ranges—are shown in the histogram illustrated in Fig. 11.

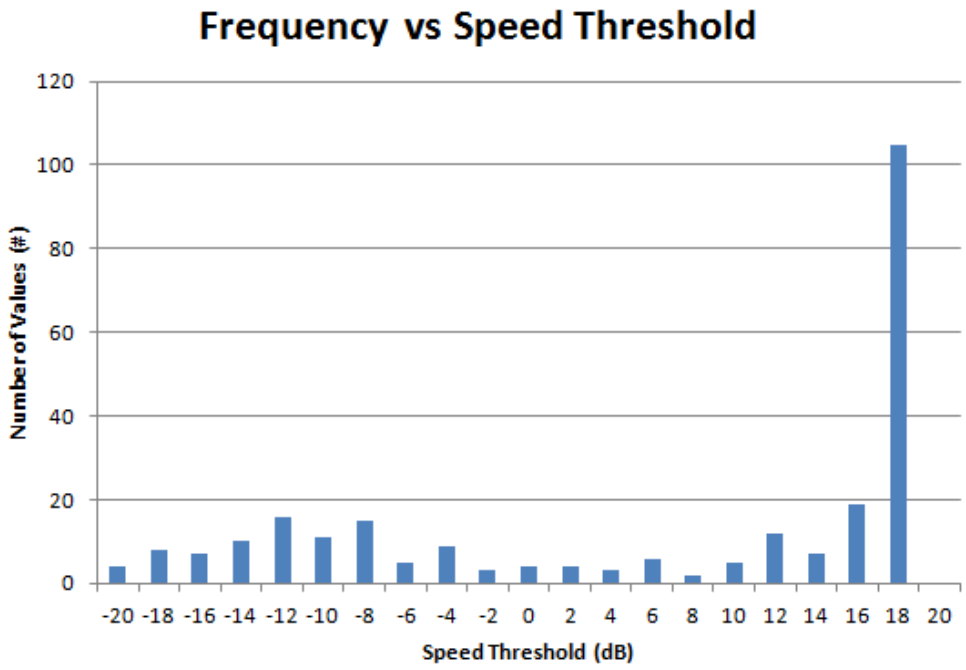


**Fig. 11 Histogram of all threshold values obtained in the study**

Figure 11 shows behaviors consistent with the simulation results shown in Fig. 8. A large number of trials resulted in values at the upper limit of our experimental range. The simulated results of Fig. 8 indicate that the values in Fig. 11— in the range between 18 and 20 dB plotted above the 18-dB value—are due to MVT values above 20 dB or beyond visible limits altogether.

At the lower limit of our experimental range, Fig. 11 shows a decrease in the number of measured thresholds as the movement rate approaches –20 dB. This indicates that, unlike the number of MVT values above domain limit or possibly undefined, only a few participants had MVT values that might be below the experimental domain. This shows that we adequately captured the lower limit of motion detection at 40° eccentricity; we presented movement so slow that even if people could see the targets, most participants could not detect target movement at the slowest rates presented. Thus, we generally presented motion slow enough to not be seen by test participants.

Figure 11 also shows a local minimum number of MVT measurements between –2 and 8 dB. MVT values are more prevalent at movement rates from –20 to –2 dB than at movement rates from –2 to 8 dB. For movement rates above –2 dB, our measurements indicate that people general can no longer see movement at any eccentricities or ranges.

Figure 12 shows the distribution of MVT values greater than –20 dB and less than 4 dB.

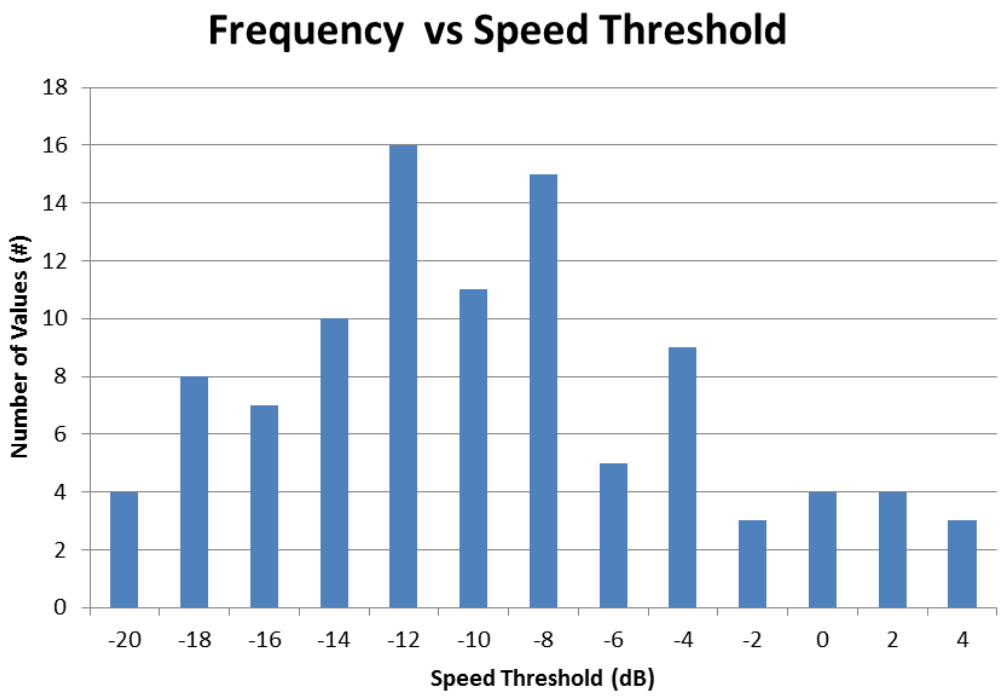


**Fig. 12 Histogram of MVT values greater than –20 dB and less than 4 dB**

At the upper range of our experimental domain, the similarity in MVT value distributions in Figs. 8 and 11 indicate that MVT measurements above a value of approximately 10 dB may be due to out-of-range MVT values or targets that could not be seen at all, regardless of movement rate. In the range below –2dB, the average of the MVT values is approximately –10 dB.

There is no precise separation point between actually observed MVT values and MVT values resulting from the QUEST procedure when the actual MVT value was above our experimental domain or when the target could not be seen regardless of motion. We can only estimate an average separation point across all subjects. Our data have a local minimum at 8 dB, and a separation estimate may be as low as –2 dB or as high as 8 dB. Neural imaging may present an experimental procedure to further refine this estimate for individual participants.

Overall, our combined data indicate that the distributions of MVTs for human peripheral vision extend from a minimum value near –20 dB to an upper limit possibly between –2 and 8 dB, and the distribution has an average value of approximately –11 dB for eccentricities between 40° and 80° for targets representing human form shadows with a target contrast of –0.2.

We calculated the average and standard deviation of the human threshold distribution for motion detection as a function of eccentricity and range for the targets and conditions of our study.

Average and standard deviation MVTs across all participants are shown in Table 2. In Table 1, eccentricity values are in the red region, range values are in the yellow region, and average and standard deviation MVT values are in the green region

**Table 1 Average and standard deviation MVTs across all participants**

| Average and ± standard deviation MVT results (dB) | | Range (m) | | |
|---|---|---|---|---|
| | | 50 | 100 | 200 |
| Eccentricity (°) | 40 | –13.0 ± 2.5 | –5.4 ±3.0 | 9.4 ± 4.7 |
| | 50 | –10.9 ± 4.1 | –0.8 ±5.6 | 16.0 ± 3.4 |
| | 60 | –9.4 ± 4.1 | 10.4 ±5.8 | 17.8 ± 1.3 |
| | 70 | 4.5 ± 5.6 | 17.7 ±2.0 | 18.0 ± 1.0 |
| | 80 | 17.8 ± 2.5 | 18.2 ±1.3 | 17.4 ± 1.7 |

Table 1 shows a decrease in standard deviation for MVT distributions with averages below –11 dB and above 15 dB. As noted earlier, measurements above a value of approximately 10 dB may be due to out-of-range MVT values or targets that could not be seen at all regardless of movement rate.

Average MVTs across all participants are shown as a function of range and eccentricity by the MVT surface in Fig. 13.

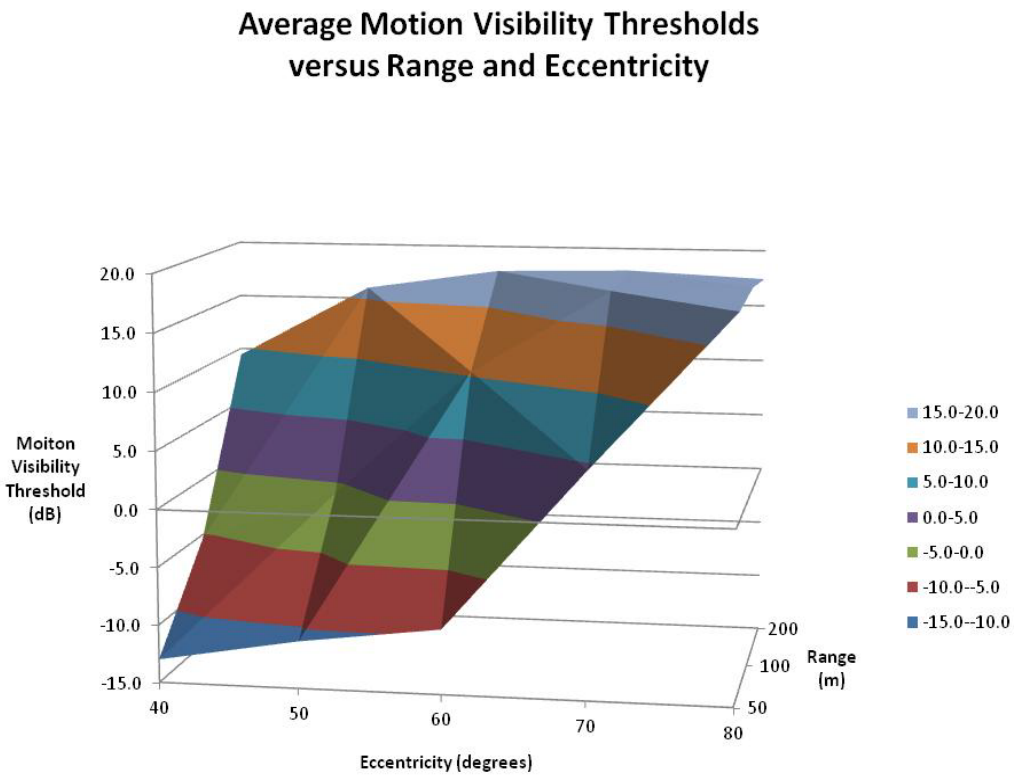


**Fig. 13 Average MVT surface as a function of eccentricity and range**

The lowest average MVT value is at 40° eccentricity (the lowest eccentricity value) and 50-m range (the lowest value in the range variable). The upper limit of real MVT values remains imprecise. Figure 13 indicates the shape of a real movement visibility threshold surface between –15 and +10 dB. Above about 10 dB, the QUEST procedure was more than 5% likely to have simply been converging on the maximum threshold in our study.

To help illustrate the dependence of the MVT on range and eccentricity, we plot MVT as a function of one independent variable for each separate value of the other independent variable in Figs. 14 and 15.

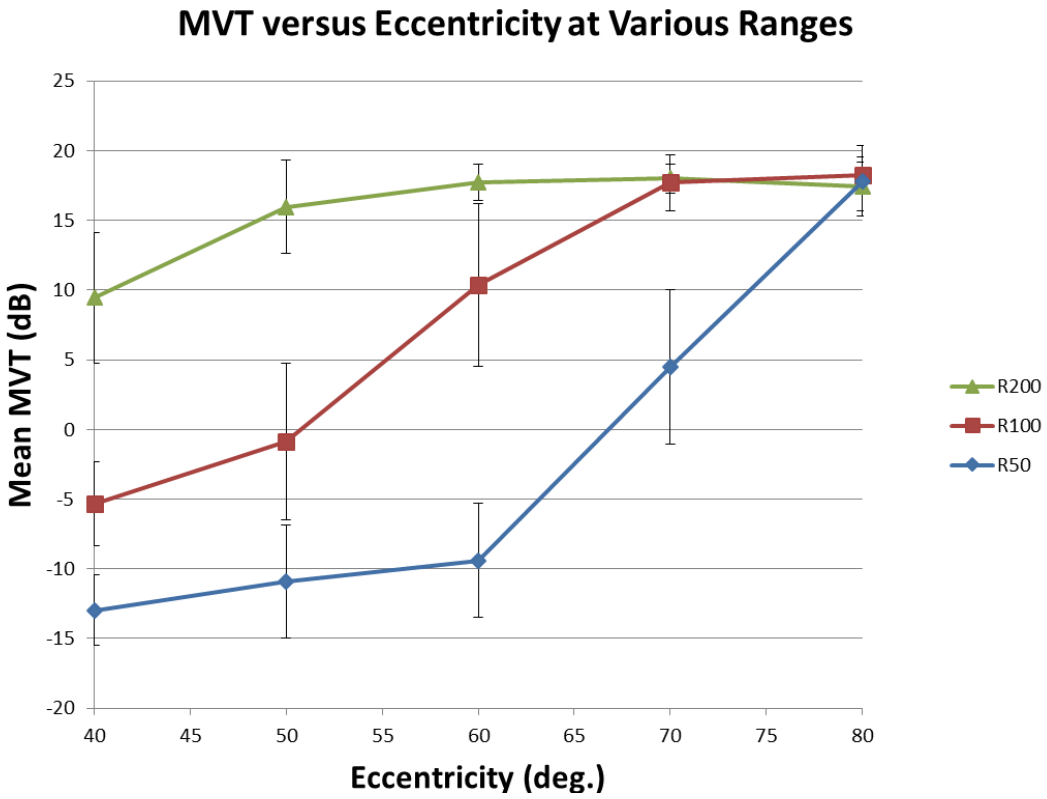


**Fig. 14 MVT vs. eccentricity at ranges of 200, 100, and 50 m with error bars showing the standard deviation estimated for the MVT distribution at each eccentricity-range combination**

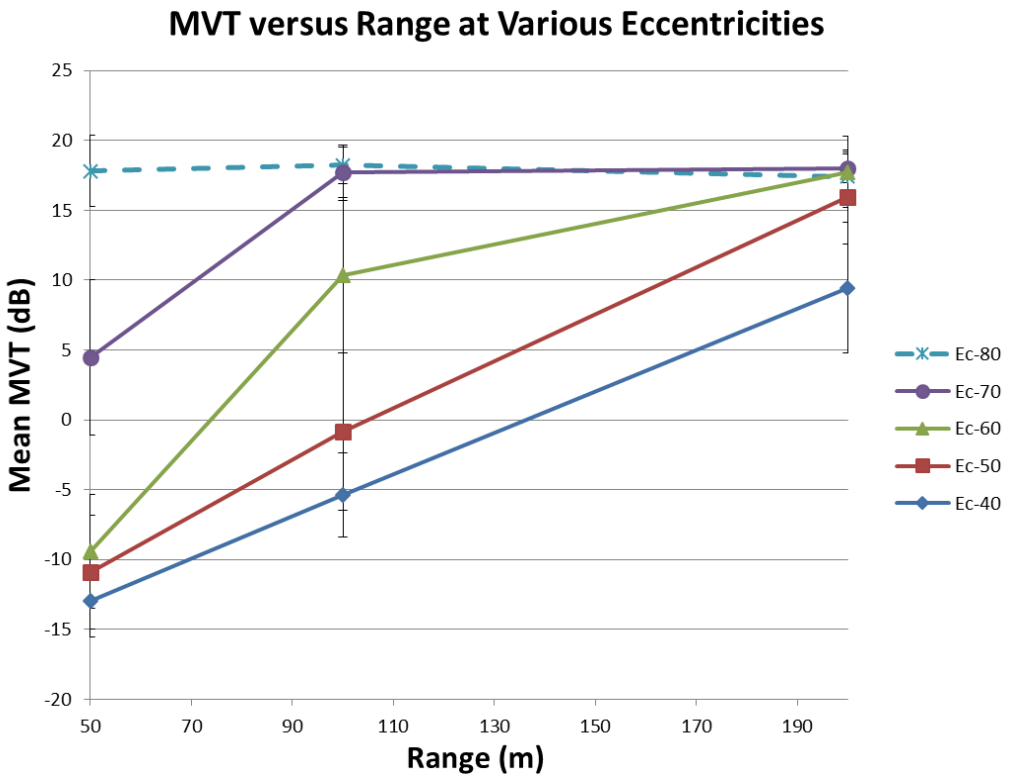


**Fig. 15 MVT vs. range at eccentricities of 80°, 70°, 60°, 50°, and 40° at each eccentricity with error bars showing the standard deviation estimated for the MVT distribution at each eccentricity-range combination**

Figure 14 shows the dependence of thresholds on eccentricity for various ranges. Measurements of rates above 10 dB may be biased by individual thresholds that were beyond the 20-dB maximum range of our study or by MVT values that unbounded because targets could not be seen regardless of motion. This bias is also indicated by the 95% confidence intervals for mean MVTs at each range and eccentricity. The confidence intervals decrease as the threshold values plateau toward the maximum motion rate. Since we have no reason to expect confidence intervals to decrease, this decrease is an indication that the QUEST procedure was converging at the upper experimental limit.

Again, as the MVT averages rise, the upper experimental limit appears to restrict the QUEST values. The values of MVT above 10 dB remain uncertain. As the dashed line for an eccentricity of 80° shows, MVT thresholds for all ranges at that eccentricity are either above the limit of our experimental range or the thresholds are nonexistent because the targets could not be seen regardless of movement.

As an example of the application of these measurements, we consider a person running with a speed of 4 $m \cdot s^{-1}$. Table A-2 in the Appendix shows that this speed corresponds to 2 dB at 50 m, –4 dB at 100 m, and –10 dB at 200 m. Figure 14 shows a range of 50 m with a movement equivalent to 2 dB. A target of human size and

form moving with this running speed could be visually detected by this movement at eccentricities less than 60°–70°. If movement were at 100 m with a movement equivalent to –4 dB, detection of this movement would likely occur only at peripheral angles less than 45°. At 200 m, with a movement equivalent to –10 dB, this motion would go undetected at all peripheries greater than 40°.

## 5. Conclusion

This research provides initial estimates of motion sensitivity in the far periphery. Target size and target contrast were selected from recommendations for representing humans as they may appear in some battle environments. Targets approximate the human form at ranges from 50 to 200 m, and lighting conditions produced a Michelson contrast of –0.2 darkened with respect to the background.

It is useful to compare our results with those obtained by Monaco et al. (2007), who reported MVTs of $1.35°\cdot s^{-1}$ at 72.5° eccentricity and $2.3°\cdot s^{-1}$ at 90° eccentricity. Our threshold visibilities values are much larger: approximately $6°\cdot s^{-1}$ at 70° eccentricity and above $36°\cdot s^{-1}$, if not nonexistent, at 80° eccentricities. We attribute the difference to the difference between the contrasts of the stimuli used in the studies. We applied a recommended Michelson contrast of –0.2, while Monaco et al. applied a contrast estimated to be –0.97, which is much greater. We also used Gabor patch targets, which lack sharply defined edges, while Monaco et al. applied solid black targets on white backgrounds.

Measured MVT values can be used to develop a Soldier behavioral target-searching strategy that includes deviations from a rigid rasterized target-search process. The deviations can be based on target movement cues that direct foveal attention toward an object when the object moves at angular rates above the threshold at the appropriate visual eccentricity and target range within the Soldier's field of view.

Further research is required to better refine the upper limits of movement visibility thresholds at larger values of eccentricity. Further measurements also may help resolve absolute limits of movement detection at increasing eccentricities, where the target cannot be seen regardless of its rate of movement. Also, further measurements are needed to determine how MVTs depend on contrast and target edge thickness. Regardless, incorporating motion-cued target detection in Solder visual performance modeling will provide a model of the human performance based on behavioral characteristics as Soldiers search for enemy combatants, and the motion visibility estimates provided in this report can form visibility hypotheses that can be tested in the field.

## 6. References


Anstis S, Verstraten FAJ, Mather G. Trends in cognitive science. 1998;2(3):111–117.

Brooks BE, Cooper EE. What types of visual recognition tasks are mediated by the neural subsystem that subserves face recognition? Journal of Experimental Psychology: Learning Memory and Cognition. 2006;32:684–698.

Fouts WR, Nelson DR. Prey capture by the Pacific angel shark, *Squatina Californica*: visually mediated strikes and ambush-site characteristics. Copeia. 1999;2:304–312.

Hood DC, Finkelstein MA. Sensitivity to light. In: Boff K, Kaufman L, Thomas J, editors. Handbook of perception and human performance; vol. 1: sensory processes and perception. New York (NY): John Wiley and Sons; 1986.

Ioannou CC, Krause J. Interactions between background matching and motion during visual detection can explain why cryptic animals keep still. Biology Letters. 2009;5(2):191–193.

Johnson J. Analysis of image forming systems. In: Johnson RB, Wolfe WL, editors. Selected papers on infrared design, part one and part two. Bellingham (WA): SPIE-The International Society for Optical Engineering; 1985. p. 761.

Jonides J. Voluntary versus automatic control over the mind's eye's movement. In: Long JB, Baddeley AD, editors. Attention and performance IX. Hillsdale (NJ): Lawrence Erlbaum Associates Inc.; 1981. p. 187–203.

King-Smith PE, Grigsby SS, Vingrys AJ, Benes SC, Supowit A. Efficient and unbiased modifications of the QUEST threshold method: theory, simulations, experimental evaluation and practical implementation. Vision Research. 1994;34:885–912.

Klein SA. Measuring, estimating, and understanding the psychometric function: a commentary. Perception & Psychophysics. 2001;63:1421–1455.

McKee SP, Nakayama K. The detection of motion in the peripheral visual field. Vision research. 1984;24(1):25-32.

Monaco WA, Higgins KE, Kalb JT. Central and off-axis spatial contrast sensitivity measured with Gabor patches. Aberdeen Proving Ground (MD): Army Research Laboratory (US); 2010. Report No.: ARL-TR-5363.

Monaco WA, Kalb JT, Johnson CA. Motion detection in the far peripheral visual field. Aberdeen Proving Ground (MD): Army Research Laboratory (US); 2007. Report No.: ARL-MR-0684.

Peli E, Arend L. Contrast sensitivity to patch stimuli: effects of spatial bandwidth and temporal presentation. Spatial Vision. 1993;7:1–14.

Peli E. In search of a contrast metric: matching the perceived contrast of Gabor patches at different phases and bandwidths. Vision Research. 1997;37:3217–3224.

Ratches JA, Vollmerhausen RH, Driggers RG. Target acquisition performance modeling of infrared imaging systems: past, present, and future. IEEE Sensors Journal. 200;1:31–40.

Rauschenberger R. Attentional capture by auto- and allo-cues. Psychological Bulletin and Review. 2003;10:841–842.

Taylor MM, Creelman CD. PEST: efficient estimates on probability functions. J Acoust Soc Am. 1967;41(4):782–787.

TransAnalytics LLC. Summary of medical advisory board practices in the United States; 2003 [accessed 2013 Jan 14]. http://www.mdsupport.org /drivingsummary.pdf.

US Department of the Army use of volunteers as subjects of research. Washington (DC): Government Printing Office (US); 1990. Report No.: AR 70-25

Venezia JD. Operations Research Analyst, US Army Natick Research, Development and Evaluation Center. Personal communication; 2009 July 8.

Watson AB Pelli DG. QUEST: a Bayesian adaptive psychometric method. Perception & Psychophysics. 1983;33:113–120.

Weyand PG, Sternlight DB, Bellizzi MJ, Wright S. Faster top running speeds are achieved with greater ground forces not more rapid leg movements. J Appl Physiol. 2000;89:(5)1991.

Yantis S, Hillstrom AP. Visual motion and attentional capture. Perception & Psychophysics. 1994;55:399–411.

Yantis S. Attentional capture in vision. In: Kramer A, Coles M, Logan G, editors. Converging operations in the study of selective visual attention. Washington (DC): American Psychological Association; 1996. p. 45–76.

# Appendix. Angular Displacement Rates and Equivalent Speeds for Target Eccentricities and Ranges

Table A-1 gives angular displacements in degrees per second at each eccentricity angle.

**Table A-1 Angular displacement rates (°•s$^{-1}$) for target eccentricities**

| Target speed | Angle (°) | Angle (°) | Angle (°) | Angle (°) | Angle (°) |
|---|---|---|---|---|---|
| Level | 40 | 50 | 60 | 70 | 80 |
| dB | °•s$^{-1}$ | °•s$^{-1}$ | °•s$^{-1}$ | °•s$^{-1}$ | °•s$^{-1}$ |
| 20 | 3.19E+01 | 3.51E+01 | 3.62E+01 | 3.51E+01 | 3.19E+01 |
| 19 | 2.85E+01 | 3.13E+01 | 3.22E+01 | 3.13E+01 | 2.85E+01 |
| 18 | 2.54E+01 | 2.79E+01 | 2.87E+01 | 2.79E+01 | 2.54E+01 |
| 17 | 2.26E+01 | 2.48E+01 | 2.56E+01 | 2.48E+01 | 2.26E+01 |
| 16 | 2.02E+01 | 2.21E+01 | 2.28E+01 | 2.21E+01 | 2.02E+01 |
| 15 | 1.80E+01 | 1.97E+01 | 2.03E+01 | 1.97E+01 | 1.80E+01 |
| 14 | 1.60E+01 | 1.76E+01 | 1.81E+01 | 1.76E+01 | 1.60E+01 |
| 13 | 1.43E+01 | 1.57E+01 | 1.62E+01 | 1.57E+01 | 1.43E+01 |
| 12 | 1.27E+01 | 1.40E+01 | 1.44E+01 | 1.40E+01 | 1.27E+01 |
| 11 | 1.13E+01 | 1.25E+01 | 1.28E+01 | 1.25E+01 | 1.13E+01 |
| 10 | 1.01E+01 | 1.11E+01 | 1.14E+01 | 1.11E+01 | 1.01E+01 |
| 9 | 9.00E+00 | 9.89E+00 | 1.02E+01 | 9.89E+00 | 9.00E+00 |
| 8 | 8.03E+00 | 8.81E+00 | 9.09E+00 | 8.81E+00 | 8.03E+00 |
| 7 | 7.15E+00 | 7.86E+00 | 8.10E+00 | 7.86E+00 | 7.15E+00 |
| 6 | 6.37E+00 | 7.00E+00 | 7.22E+00 | 7.00E+00 | 6.37E+00 |
| 5 | 5.68E+00 | 6.24E+00 | 6.43E+00 | 6.24E+00 | 5.68E+00 |
| 4 | 5.06E+00 | 5.56E+00 | 5.73E+00 | 5.56E+00 | 5.06E+00 |
| 3 | 4.51E+00 | 4.96E+00 | 5.11E+00 | 4.96E+00 | 4.51E+00 |
| 2 | 4.02E+00 | 4.42E+00 | 4.55E+00 | 4.42E+00 | 4.02E+00 |
| 1 | 3.58E+00 | 3.94E+00 | 4.06E+00 | 3.94E+00 | 3.58E+00 |
| 0 | 3.19E+00 | 3.51E+00 | 3.62E+00 | 3.51E+00 | 3.19E+00 |
| –1 | 2.85E+00 | 3.13E+00 | 3.22E+00 | 3.13E+00 | 2.85E+00 |
| –2 | 2.54E+00 | 2.79E+00 | 2.87E+00 | 2.79E+00 | 2.54E+00 |
| –3 | 2.26E+00 | 2.48E+00 | 2.56E+00 | 2.48E+00 | 2.26E+00 |
| –4 | 2.02E+00 | 2.21E+00 | 2.28E+00 | 2.21E+00 | 2.02E+00 |
| –5 | 1.80E+00 | 1.97E+00 | 2.03E+00 | 1.97E+00 | 1.80E+00 |
| –6 | 1.60E+00 | 1.76E+00 | 1.81E+00 | 1.76E+00 | 1.60E+00 |
| –7 | 1.43E+00 | 1.57E+00 | 1.62E+00 | 1.57E+00 | 1.43E+00 |
| –8 | 1.27E+00 | 1.40E+00 | 1.44E+00 | 1.40E+00 | 1.27E+00 |
| –9 | 1.13E+00 | 1.25E+00 | 1.28E+00 | 1.25E+00 | 1.13E+00 |
| –10 | 1.01E+00 | 1.11E+00 | 1.14E+00 | 1.11E+00 | 1.01E+00 |
| –11 | 9.00E-01 | 9.89E-01 | 1.02E+00 | 9.89E-01 | 9.00E-01 |
| –12 | 8.03E-01 | 8.81E-01 | 9.09E-01 | 8.81E-01 | 8.03E-01 |
| –13 | 7.15E-01 | 7.86E-01 | 8.10E-01 | 7.86E-01 | 7.15E-01 |
| –14 | 6.37E-01 | 7.00E-01 | 7.22E-01 | 7.00E-01 | 6.37E-01 |
| –15 | 5.68E-01 | 6.24E-01 | 6.43E-01 | 6.24E-01 | 5.68E-01 |
| –16 | 5.06E-01 | 5.56E-01 | 5.73E-01 | 5.56E-01 | 5.06E-01 |
| –17 | 4.51E-01 | 4.96E-01 | 5.11E-01 | 4.96E-01 | 4.51E-01 |
| –18 | 4.02E-01 | 4.42E-01 | 4.55E-01 | 4.42E-01 | 4.02E-01 |
| –19 | 3.58E-01 | 3.94E-01 | 4.06E-01 | 3.94E-01 | 3.58E-01 |
| –20 | 3.19E-01 | 3.51E-01 | 3.62E-01 | 3.51E-01 | 3.19E-01 |

Table A-2 gives the velocity of movement at each range. Velocities are shown for the 60° eccentricity. Velocities at other eccentricities are approximately equal to the velocity at 60° eccentricity.

To add perspective to the velocities in the tables, the velocity values are color-shaded to represent the following approximate ranges:

- Green: human walking speeds; velocity <2.24 $m \cdot s^{-1}$ (5 mph)
- Yellow: human running speeds; 2.24 $m \cdot s^{-1}$ (5 mph) < velocity < 8.94 $m \cdot s^{-1}$ (20 mph)
- Red: vehicle driving speeds; velocity >8.94 $m \cdot s^{-1}$ (20 mph)

**Table A-2 Velocity at ranges for 60° eccentricity**

| Target speed (mph) | Range (m) | Range (m) | Range (m) |
|---|---|---|---|
| Level | 50 | 100 | 200 |
| dB | m/s | m/s | m/s |
| 20 | 31.57 | 63.15 | 126.30 |
| 19 | 28.14 | 56.28 | 112.56 |
| 18 | 25.08 | 50.16 | 100.32 |
| 17 | 22.35 | 44.71 | 89.41 |
| 16 | 19.92 | 39.84 | 79.69 |
| 15 | 17.76 | 35.51 | 71.02 |
| 14 | 15.82 | 31.65 | 63.30 |
| 13 | 14.10 | 28.21 | 56.41 |
| 12 | 12.57 | 25.14 | 50.28 |
| 11 | 11.20 | 22.41 | 44.81 |
| 10 | 9.98 | 19.97 | 39.94 |
| 9 | 8.90 | 17.80 | 35.59 |
| 8 | 7.93 | 15.86 | 31.72 |
| 7 | 7.07 | 14.14 | 28.27 |
| 6 | 6.30 | 12.60 | 25.20 |
| 5 | 5.61 | 11.23 | 22.46 |
| 4 | 5.00 | 10.01 | 20.02 |
| 3 | 4.46 | 8.92 | 17.84 |
| 2 | 3.97 | 7.95 | 15.90 |
| 1 | 3.54 | 7.09 | 14.17 |
| 0 | 3.16 | 6.31 | 12.63 |
| –1 | 2.81 | 5.63 | 11.26 |
| –2 | 2.51 | 5.02 | 10.03 |
| –3 | 2.24 | 4.47 | 8.94 |
| –4 | 1.99 | 3.98 | 7.97 |
| –5 | 1.78 | 3.55 | 7.10 |
| –6 | 1.58 | 3.16 | 6.33 |
| –7 | 1.41 | 2.82 | 5.64 |
| –8 | 1.26 | 2.51 | 5.03 |
| –9 | 1.12 | 2.24 | 4.48 |
| –10 | 1.00 | 2.00 | 3.99 |
| –11 | 0.89 | 1.78 | 3.56 |
| –12 | 0.79 | 1.59 | 3.17 |
| –13 | 0.71 | 1.41 | 2.83 |
| –14 | 0.63 | 1.26 | 2.52 |
| –15 | 0.56 | 1.12 | 2.25 |
| –16 | 0.50 | 1.00 | 2.00 |
| –17 | 0.45 | 0.89 | 1.78 |
| –18 | 0.40 | 0.79 | 1.59 |
| –19 | 0.35 | 0.71 | 1.42 |
| –20 | 0.32 | 0.63 | 1.26 |

## List of Symbols, Abbreviations, and Acronyms

| | |
|---|---|
| 2-D | 2-dimensional |
| AMSAA | US Army Materiel Systems Analysis Activity |
| ARL | US Army Research Laboratory |
| $cd/m^2$ | candelas per square meter |
| IP | Internet Protocol |
| IR | infrared |
| IWARS | Infantry Warrior Simulation |
| MVT | motion visibility threshold |
| NSRDEC | US Army Natick Soldier Research, Development and Engineering Center |
| PC | personal computer |
| PD | probability distribution |
| PEST | Parameter Estimation by Sequential Testing |
| RGB | red-green-blue |
| TESF | Tactical Environment Simulation Facility |
| TP | test participant |

1 (PDF) DEFENSE TECHNICAL INFORMATION CTR DTIC OCA

2 (PDF) DIRECTOR US ARMY RESEARCH LAB RDRL CIO L IMAL HRA MAIL & RECORDS MGMT

1 (PDF) GOVT PRINTG OFC A MALHOTRA

1 (PDF) ARMY RSCH LAB – HRED RDRL HRB B T DAVIS BLDG 5400 RM C242 REDSTONE ARSENAL AL 35898-7290

1 (PDF) ARMY RSCH LAB – HRED RDRL HRB A R SPENCER BLDG E2929 DESERT STORM DR FORT BRAGG NC 28310-0001

8 (PDF) ARMY RSCH LAB – HRED SFC PAUL RAY SMITH CTR RDRL HRO COL H BUHL RDRL HRF J CHEN RDRL HRA I MARTINEZ RDRL HRR R SOTTILARE RDRL HRA C A RODRIGUEZ RDRL HRA B G GOODWIN RDRL HRA A C METEVIER RDRL HRA D B PETTIT 12423 RESEARCH PARKWAY ORLANDO FL 32826

1 (PDF) USA ARMY G1 DAPE HSI B KNAPP 300 ARMY PENTAGON RM 2C489 WASHINGTON DC 20310-0300

1 (PDF) USAF 711 HPW 711 HPW/RH K GEISS 2698 G ST BLDG 190 WRIGHT PATTERSON AFB OH 45433-7604

1 (PDF) USN ONR ONR CODE 341 J TANGNEY 875 N RANDOLPH STREET BLDG 87 ARLINGTON VA 22203-1986

1 (PDF) USA NSRDEC RDNS D D TAMILIO 10 GENERAL GREENE AVE NATICK MA 01760-2642

1 (PDF) OSD OUSD ATL HPT&B B PETRO 4800 MARK CENTER DRIVE SUITE 17E08 ALEXANDRIA VA 22350

ABERDEEN PROVING GROUND

15 (PDF) DIR USARL RDRL DPT K KEHRING RDRL HR J LOCKETT P FRANASZCZUK K MCDOWELL K OIE RDRL HRB D HEADLEY RDRL HRB BA B VAUGHN RDRL HRB C J GRYNOVICKI RDRL HRB D C PAULILLO RDRL HRF A A DECOSTANZA RDRL HRF B A EVANS RDRL HRF C J GASTON P FEDELE RDRL HRF D A MARATHE RDRL LOC I A KALB